Acta Pharmacologica Sinica 2017: 1009–1023
 1671-4083/17
www.nature.com/aps

Original Article

LY333531, a PKCβ inhibitor, attenuates glomerular endothelial cell apoptosis in the early stage of mouse diabetic nephropathy via down-regulating swiprosin-1

Zhi-bin WANG[1, #], Su ZHANG[2, #], Ya LI[1, #], Rong-mei WANG[1], Ling-chang TONG[1], Yue WANG[3], Wei-ye LIU[1], Ding-feng SU[1], Ye TU[4, *], Li-chao ZHANG[2, 3, *], Ling LI[1, *]

[1]Department of Pharmacology, College of Pharmacy, Second Military Medical University, Shanghai 200433, China; [2]Department of Pharmacy, Ningxia Medical University, Yinchuan 750021, China; [3]Department of Pharmacy, Shanghai Municipal Hospital of Traditional Chinese Medicine, Shanghai 200071, China; [4]Medical Affairs Department, Shanghai East Hospital, Tongji University, Shanghai 200120, China

Abstract

Glomerular endothelial cell (GEC) injury plays an important role in the early stage of diabetic nephropathy (DN). Previous studies show that a PKCβ inhibitor is effective for treating DN. In the current study we further explored the effects and molecular mechanisms of PKCβ inhibitors on GEC apoptosis in DN in streptozotocin-induced diabetic mice *in vivo* and high glucose- or PMA-treated human renal glomerular endothelial cells (HRGECs) *in vitro*. In the diabetic mice, hyperglycemia caused aggravated nephropathy and GEC apoptosis accompanied by significantly increased expression of swiprosin-1, a potentially pro-apoptotic protein. Administration of LY333531 (1 $mg{\cdot}kg^{-1}{\cdot}d^{-1}$ for 8 weeks) significantly attenuated both GEC apoptosis and swiprosin-1 upregulation in the diabetic mice. Similar results were observed in high glucose- or PMA-treated HRGECs *in vitro*. The pro-apoptotic role of swiprosin-1 was further examined using HRGECs treated with lentivirus mediating RNA interference or over-expression and swiprosin-1-knockout mice. Over-expression of swiprosin-1 in HRGECs resulted in increases in apoptosis and in caspase-9, caspase-3 and Bax expression. In contrast, knockdown of swiprosin-1 attenuated high glucose- or PMA-induced HRGECs apoptosis. Furthermore, over-expression of swiprosin-1 promoted interaction between swiprosin-1 and caspase-9 and increased the formation of apoptosomes. In diabetic *swiprosin-1*$^{-/-}$ mice, the kidney/body weight, urinary albumin, glomerular hypertrophy, mitochondrial apoptotic-associated proteins and GEC apoptosis were significantly attenuated as compared with those in diabetic *swiprosin-1*$^{+/+}$ mice. These results demonstrate that swiprosin-1 is up-regulated by PKCβ in the early stage of DN, and that PKCβ facilitates GEC apoptosis through the mitochondrial-dependent pathway.

Keywords: LY333531; diabetic nephropathy; glomerular endothelial cells; PKCβ; PMA; swiprosin-1; apoptosis

Acta Pharmacologica Sinica (2017) 38: 1009–1023; doi: 10.1038/aps.2016.172; published online 10 Apr 2017

Introduction

Diabetic nephropathy (DN) is the leading cause of end stage renal disease and leads to disabilities and high mortality rates in patients with diabetes[1, 2]. Glomerular abnormalities, such as glomerular hyperfiltration and increased albuminuria excretion, in the early stage of DN are important steps in the development of DN. These pathological changes are, in part, the consequences of glomerular damage[3]. The glomerulus is a capillary network that is primarily composed of endothelial cells, podocytes and mesangial cells. The classical histological features of early stage of DN include mesangial expansion and glomerular basement membrane thickening, accompanied by podocyte detachment[4]. Previous studies have investigated how specific features, including podocyte loss, inhibition of podocytes and/or mesangial cell damage, protect against DN[5–9]. However, knowledge regarding glomerular endothelial behavior in DN is sparse. Recent accumulating evidence suggests that glomerular endothelial cell (GEC) damage is already present when podocyte injury starts. Endothelial injury in diabetes is accompanied by structural abnormalities

# These authors contributed equally to this work.
*To whom correspondence should be addressed.
E-mail lingli_z163@163.com (Ling LI);
changhaiskin@163.com (Li-chao ZHANG);
dan16065@163.com (Ye TU)
Received 2016-09-06 Accepted 2016-12-28

in the endothelium. For instance, impairment of the endothelial glycocalyx and loss of endothelial fenestrations are features of early diabetes[10]. Genetic targeting of specific genes in mice that induce endothelial injury accelerates the development of DN[11]. It was also reported that high glucose could directly induce glomerular endothelial cell apoptosis, which might contribute to glomerular endothelial injury[3]. However, the effect and mechanism of GEC apoptosis during the early stage of DN remain unclear.

Protein kinase C (PKC) is a family of serine/threonine-specific protein kinases that comprises PKC α, β_1, β_2, γ, δ, ε, θ, η, λ/ι, and ζ. Among the various signaling kinases, the PKC family plays a critical role in the pathogenesis of DN[12]. The activation of PKC in the kidney is a well-known pathway in diabetic mellitus, and it is involved in cell proliferation, differentiation, and apoptosis[13]. Among all the PKC isoforms, the role of PKCβ in the pathogenesis of DN has been investigated the most intensively. It has been demonstrated that PKCβ was increased or activated in diabetic glomeruli and contributed to glomerular hypertrophy and extracellular matrix expansion. Previous studies have shown that LY333531 (a PKCβ-selective inhibitor) blocked apoptosis in smooth muscle cells and mesangial cells under high-glucose conditions[14–16]. However, the effect and molecular mechanism of this PKCβ inhibitor on GEC apoptosis in DN have not yet been fully elucidated.

Swiprosin-1, which was first identified in lymphocytes, consists of an N-terminal region harboring a Src homology 3 (SH3) binding domain, followed by two EF-hand calcium-binding domains and a coiled-coil domain[17]. Swiprosin-1 has a medium expression level in human renal glomeruli, but it is not found in the tubules. Here, we also found that swiprosin-1 was primarily distributed in GECs and was up-regulated in diabetic mice. It has been reported that ectopic expression of swiprosin-1 in the immature murine B-cell line WEHI231 enhanced spontaneous and BCR-induced apoptosis[18]. Thylur *et al* reported that swiprosin-1 expressed in mast cells was up-regulated through $PKC\beta_1$[19]. We hypothesized that activation of PKCβ could enhance swiprosin-1 expression and mediate GEC apoptosis in the early stage of DN.

In this study, we first sought to investigate whether GEC apoptosis was regulated by PKCβ in glomeruli of diabetic mice and in human renal glomerular endothelial cells (HRGECs) treated with high glucose. To elucidate the role of swiprosin-1 in the early stage of DN, we examined whether the expression of swiprosin-1 was regulated by PKCβ *in vivo* and *in vitro*. Moreover, we examined whether and how swiprosin-1 facilitated GEC apoptosis *in vivo* and *in vitro*.

Materials and methods

Diabetes model

All mice used in this study were on a congenic C57BL/6 background. At 8 weeks of age, male mice were intraperitoneally injected with a single dose of streptozotocin (STZ) (150 mg/kg; Sigma-Aldrich, St Louis, MO, USA) or sodium citrate vehicle[20]. After 72 h, diabetes was confirmed in STZ-treated mice by measuring tail vein plasma glucose (random blood glucose value >16.7 mmol/L). At the end of the experiment, the mice were killed and blood and kidneys were harvested. Twelve-hour urine samples were collected on the day before euthanasia by housing the animals in metabolic cages to determine the urine albumin excretion rate[21]. All mice were maintained under an automated 12 h/12 h dark-light cycle at a controlled temperature of 22±2 °C and a relative humidity of 50%–60% and were allowed free access to a standard dry diet and tap water *ad libitum*. All protocols were approved by the Animal Care Committee at the Second Military University.

Cell culture

HRGECs were obtained from ScienCell Research Laboratories, Santiago, CA, USA, and cultured according to the instructions. Briefly, cells were grown on 2 μg/cm^2 fibronectin-coated plates and maintained at 37 °C in a humidified 5% CO_2 incubator using endothelial cell medium (ScienCell Research Laboratories) in the presence of growth factors and supplements. The cells in experiments were used within 4 passages.

Generation of swiprosin-1-deficient mice

Recombineering was used to generate a gene targeting construct from a bacterial artificial chromosome (BAC) containing the *swiprosin-1* gene (C57BL/6 inbred strain). E14 ES cells were transfected with this construct, and successfully targeted ES cells were injected into C57BL/6 blastocysts. Mice bearing this targeted allele with exon 2-4 deletion in the germline were bred to generate *swiprosin-1*$^{-/-}$ mice.

Lentivirus construction and preparation

Avramidou[18] used the 19-nucleotide sequence 5′-GCGTTT-GCCTCAGCGGATA-3′ (residues 2004–2022 in the murine swiprosin-1 cDNA sequence, GenBank NM_025994) as a target to construct shRNA for stable knockdown of swiprosin-1. Calculation results using Oligoengine Workstation software showed an interference efficiency of up to 80%. We selected a new 19-nucleotide sequence consisting of 5′-AAGGGTGC-CAAGAACTTCT-3′ (residues 615-633 containing the CDS sequence of swiprosin-1) based on calculations performed with Oligoengine Workstation software, which showed a higher interference efficiency of approximately 85%. The experimental interference efficiencies of these two targets were 70% and 85%, respectively. The latter showed better effectiveness and thus was used to construct LV-sh-Swi. The CDS sequence (residues 54–776 in the murine swiprosin-1 cDNA sequence, GenBank NM_025994.3) was synthesized to construct LV-Swi. The recombinant lentiviruses expressing the full-length swiprosin-1 coding sequence (LV-Swi) and the swiprosin-1 interference fragment (LV-sh-Swi) were produced by the Shanghai Innovation Biotechnology Co, Ltd. The viruses were concentrated by ultracentrifugation and titered by infection of confluent 293T cells.

PKCβ-siRNA transfection

Cells were seeded at a density of 2×10^5/well in 6-well plates, incubated overnight at 37 °C, and then transfected with 75

pmol/L *PKCβ*-siRNA (GenePharma, Shanghai, China) in Opti-MEMI Reduced Serum Medium using Lipofectamine 2000 transfection reagent. The sequences of the *PKCβ*-siRNA were 5′-GCUGCUGUAUGGACUUAUUTT-3′ and 5′- AUCUCUUC-CUCAAAGCGGCTT-3′, and the sequences of negative control siRNA were 5′-UUCUCCGAACGUGUCACGUTT-3′ and 5′-ACGUGACACGUUCGGAGAATT-3′. After 6 h, transfected cells were washed and cultured for 24 h in complete medium and then stimulated with HG or NG for 48 h before being harvested for analysis.

Measurement of apoptosis

Annexin V and propidium iodide (PI) staining was performed to assess apoptosis levels[22]. Transfected cells were plated and grown overnight until they reached 60% confluence and then treated with high glucose. After 96 h, detached cells in the medium were collected, and the remaining adherent cells were harvested by trypsinization. The cells (1×10^6) were washed with cold PBS and resuspended in 1 mL of 1×binding buffer, and then, 100 μL of cells (1×10^5) was placed into individual labeled tubes. Annexin V-APC and PI (eBioscience, Santiago, CA, USA) were added to the cellular suspension, per the manufacturer's instructions, and a fluorescent sample of 10 000 cells was analyzed by flow cytometry with a FACScan flow cytometer (Becton, Dickinson and Company, Franklin, NJ, USA). Annexin V-APC-positive cells (green fluorescence) were analyzed as apoptotic. Annexin V-APC and PI-stained cells (red fluorescence) were either in the end stage of apoptosis or undergoing necrosis and analyzed as already dead. PI-stained cells were necrotic.

Cell viability assay

Cell Counting Kit-8 (CCK-8; Beyotime, Shanghai, China) was used to measure cell viability. Cells were seeded in each well of a 96-well culture plate (5×10^3/well) and incubated overnight. The medium was then removed, and the cells were incubated for 96 h with 100 μL of experimental medium containing high glucose. Thereafter, 10 μL of CCK-8 solution was added, and cells were incubated for 1 h at 37 °C. Absorbance was measured using a microplate reader (Thermo Fisher Scientific, Waltham, MA, USA) at a wavelength of 450 nm[23]. The results were calculated as the mean values of five wells for each group, and the assay was performed in triplicate.

Pyknotic nuclei count

To quantify the number of pyknotic nuclei, a cardinal feature of apoptotic cells, HRGECs on coverslips were washed once with PBS and fixed for 20 min with freshly prepared 4% paraformaldehyde in PBS. After washing twice with PBS, the HRGECs were stained with 5 μg/mL Hoechst 33342 dye (Beyotime). The number of pyknotic nuclei were expressed as a percentage of the total number of nuclei counted ($n\geq100$ nuclei per condition)[24].

Caspase-9 activity assay

To measure caspase-9 enzyme activity, cells were treated according to the protocol of a Caspase-9 Activity Assay Kit (Beyotime). Briefly[25], caspase-9 activity was examined by cleavage of a chromogenic caspase substrate, Ac-LEHD-pNA (acetyl-Leu-Glu-His-Asp *p*-nitroanilide). Sample supernatants containing 50 μg of total protein were added to a reaction buffer containing Ac-LEHD-pNA (2 mmol/L) and incubated for 4 h at 37 °C, and then the absorbance of the cleaved form of pNA was measured at 405 nm. The specific caspase-9 activity was normalized to the total protein.

Urinary albumin

Albumin is a serum protein with a relatively small molecular weight, and it is typically the first protein observed in the urine when kidney dysfunction begins to develop. Hence, urinary albumin is a suitable marker to evaluate the severity of nephritis in mouse models. Centrifuge at 10 000 rounds per minute for 5 min to remove insoluble materials in urine samples. Dilute the supernatant 1:2000 with buffer solution. An ELISA for albumin detection was used according to the manufacturer's protocol (Mouse Urinary Albumin Detection Kit; Chondrex, Redmond, WA, USA).

Serum cystatin C assay

Cystatin C (CST3) is a non-glycosylated 13 kDa protein that is almost freely filtered through the glomerular membrane, and it is completely reabsorbed and degraded by proximal tubular cells. Serum CST3 has been shown to be an ideal marker of the glomerular filtration rate[26]. An ELISA for a mouse serum CST3 assay (Abnova, Neihu District, Taipei City, Taiwan, China) was used according to the manufacturer's protocol.

Histology

Mice were perfused with ice-cold saline and then with 4% buffered paraformaldehyde. Tissues were further fixed in 4% buffered paraformaldehyde for 2 d, embedded in paraffin and processed for sectioning. Extracellular matrix deposition in the glomeruli was assessed by hematoxylin-eosin staining (H&E staining) and periodic acid–Schiff (PAS) staining. H&E staining was used for semiquantitative evaluation of glomerular sclerosis. Glomerular sclerosis was quantified per glomerulus as follows: score 1, no change; score 2, increase in mesangial matrix predominantly in the hilar area in the glomerulus or segmental mesangial proliferation (focal/multifocal), focal lesions; score 3, increase in mesangial matrix predominantly in the hilar area in the glomerulus or global mesangial proliferation, diffuse lesions[27]. ImageJ 1.44P (Wayne Rasband, National Institutes of Health, USA) software was used to measure the percentage of PAS-positive area in the glomerular tuft. Assessment of the mesangial and glomerular cross-sectional areas was performed by pixel counts on a minimum of 10 glomeruli per section in a blinded manner, under 400× magnification (Olympus Corporation, Tokyo, Japan)[28].

Immunofluorescence

HRGECs in eight-well culture slides or kidney sections were fixed with 4% paraformaldehyde in PBS for 10 min. Block-

ing was performed with immunofluorescence buffer (PBS, 2% BSA, 10% FBS) for 1 h, followed by a 10 min incubation with a second immunofluorescence buffer (PBS, 0.4% Triton X-100). Cells/tissues were incubated with primary antibody against cytochrome *c* (Beyotime, 1:50) and swiprosin-1 (Santa Cruz Biotechnology, 1:50) for 3 h at room temperature in a humidified chamber. After washing, cells were incubated with Cy3-labeled goat anti-mouse IgG (H+L) or Alexa Fluor 488-labeled goat anti-rabbit IgG (Beyotime, 1:200) for 1 h. DAPI (Beyotime) was used for nuclear staining[29, 30]. The cells were observed using a confocal laser scanning microscope (Leica, Solms, Germany).

TUNEL staining

To detect the typical features of apoptosis, nuclear DNA was stained using terminal deoxynucleotidyl transferase dUTP nick-end labeling (TUNEL) (Beyotime). After deparaffinization, the sections were treated with proteinase K (20 μg/mL, 37 °C, 15 min) and incubated with the TUNEL reaction mixture in a moist chamber (dark, 37 °C, 1 h). The sections were counterstained with DAPI to detect the nuclei. Finally, the stained sections were embedded in sealing liquid that did not quench the fluorescence[31]. TUNEL-positive cells in the kidney were observed with a confocal laser scanning microscope (Leica). Ten fields at high magnification (400×) were randomly selected from each slice. The percentage of apoptotic cells was calculated as the ratio of the number of TUNEL-positive cells to the total number of kidney cells per field.

Western blot

Cultured HRGECs or renal cortices from mice were lysed in a protein extraction reagent (Beyotime) supplemented with protease and phosphatase inhibitor cocktail (Merck, Whitehouse Station, NJ, USA). Mitochondrial and cytosolic fractions were obtained using a Cell Mitochondria Isolation Kit (Beyotime), following the steps in the instructions. Samples with equal amounts of total protein (50 μg) were separated on an SDS-polyacrylamide gel (12%) and transferred to a nitrocellulose membrane (Pall Corporation, NY, USA). The membrane was blocked with 5% bovine serum albumin and blotted with antibody. The primary antibodies used were swiprosin-1 (Santa Cruz Biotechnology; 1:1000), cleaved caspase-9 (Cell Signaling Technology, Boston, MA, USA; 1:1000), cleaved caspase-3 (Beyotime; 1:1000), Bax (Cell Signaling Technology; 1:1000), Bcl-2 (Cell Signaling Technology; 1:1000), PARP (Beyotime; 1:1000), cytochrome *c* (Beyotime; 1:1000) and tubulin (Beyotime; 1:10 000). Protein was visualized using IRDye-conjugated anti-mouse or anti-rabbit secondary antibodies (Rockland, Limerick, PA, USA) at 1:10 000. We used an Odyssey infrared imaging system (LI-COR Biosciences) to analyze the results.

Immunoprecipitation

Approximately 500 μg of protein extract was prepared for immunoprecipitation from cells that were transfected with swiprosin-1. Extracts were incubated with anti-swiprosin-1 antibody (Santa Cruz Biotechnology, Dallas, TX, USA) or anti-procaspase-9 antibody (Proteintech, Wuhan, China) at 4 °C overnight. Thereafter, 100 μL of protein A-agarose (Invitrogen, Carlsbad, CA, USA) was added, and cell extracts were incubated at 4 °C overnight. After they were washed 3 times with PBS, bound proteins were released by boiling in 60 μL of 2× SDS loading buffer for 5 min[32]. Released proteins were examined by Western blotting with anti-swiprosin-1 antibody (Santa Cruz Biotechnology), anti-procaspase-9 antibody (Proteintech), anti-cytochrome *c* antibody (Beyotime), and anti-Apaf-1 antibody (Boster, Wuhan, China) at 1:1000. An Odyssey infrared imaging system (LI-COR Biosciences, Lincoln, NE, USA) was used to analyze the results.

Statistical analysis

Data processing was performed using SPSS software (Version 18.0 for Window, SPSS, Chicago, IL, USA) and is expressed as the mean±SD of at least three independent experiments. Statistical significance was determined using Student's *t*-test or ANOVA. A value of $P<0.05$ was considered statistically significant.

Results

Hyperglycemia triggered GEC apoptosis in diabetic mice

Diabetic mice exhibited increases in blood glucose levels and kidney/body weight but a decrease in body weight at 4, 8 and 16 weeks after STZ-mediated induction of diabetes (Table 1). Serum cystatin C (CST3) is a small protein that is almost freely filtered through the glomerular membrane, and it is completely reabsorbed and degraded by proximal tubular cells[26]. Decreased CST3 concentrations reflected an increase in the glomerular filtration rate (GFR, Table 1). Furthermore, diabetic mice showed a significant increase in urinary albumin, which was coincident with the increased GFR (Table 1). Histological analysis revealed that glomerular volume, glomerulosclerosis and extracellular matrix deposition were significantly increased in diabetic mice at 8 and 16 weeks (Figure 1A). In addition, the number of apoptotic GECs was also significantly increased in diabetic mice at 8 and 16 weeks (Figure 1A), which indicated that GEC apoptosis might have occurred in the early stage of DN.

LY333531 ameliorated DN and GEC apoptosis in diabetic mice

Diabetic mice developed pronounced albuminuria and characteristic pathological changes of DN, such as glomerular hypertrophy and extracellular matrix deposition, starting at 8 weeks after STZ treatment. To demonstrate that an increase in PKCβ is causally linked to aggravated nephropathy and GEC apoptosis in diabetic mice, a separate group was treated with LY333531 at a dose of 1 $mg \cdot kg^{-1} \cdot d^{-1}$ and euthanized 8 weeks after induction of diabetes through STZ injection. LY333531 significantly alleviated the increase in kidney/body weight, urinary albumin and GFR (Table 2). Renal cortex tissue was analyzed to identify the histopathological changes and GEC apoptosis modulated by LY333531. The PKCβ inhibitor attenuated extracellular matrix deposition and glomerulosclerosis

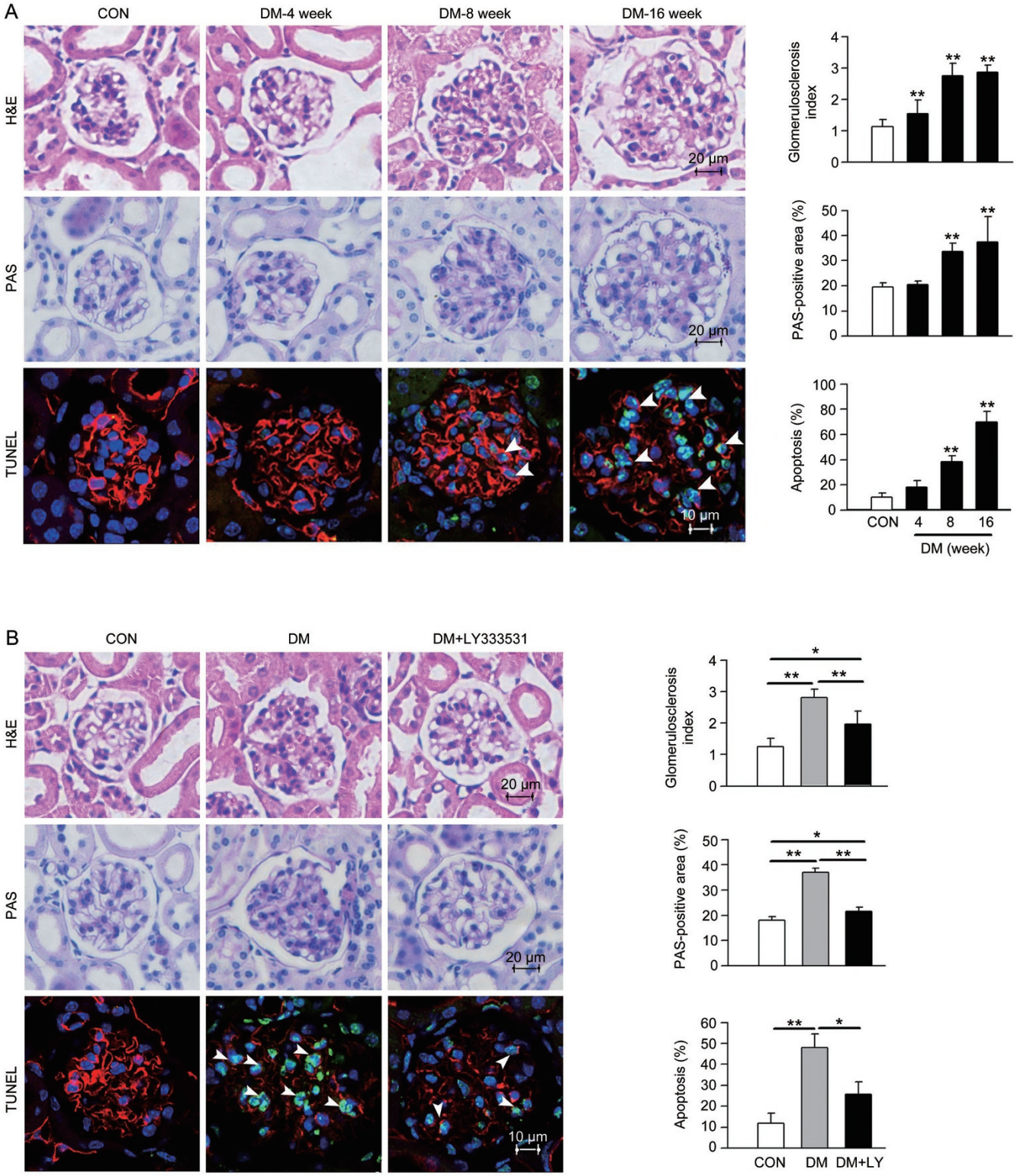

Figure 1. LY333531 ameliorated renal glomerular injury and GEC apoptosis in diabetic mice. (A) Kidney sections were treated with hematoxylin-eosin staining (H&E staining), periodic acid-Schiff staining (PAS staining), and TUNEL staining in diabetic mice at 4, 8 and 16 weeks. (B) Kidney sections were treated with H&E staining, PAS staining, and TUNEL staining in diabetic mice at 8 weeks treated with or without LY333531 (1 mg·kg^{-1}·d^{-1}). TUNEL-stained fluorescein-labeled nucleotides (green, labeled apoptotic cells); CD31 (red, labeled endothelial cells); DAPI nuclear counterstain (blue). Images are representative of 5 mice in each group. Scale bar=20 μm in H&E and PAS staining; scale=10 μm in TUNEL staining. CON, control; DM, diabetes mellitus; LY, LY333531.

and efficiently prevented GEC apoptosis (Figure 1B). These results suggested that PKCβ activation might result in GEC apoptosis to promote the progression of DN.

Swiprosin-1 expression was up-regulated through PKCβ in GECs of diabetic mice

Here, we first observed the distribution of swiprosin-1 in mouse kidney and verified extensive expression of swiprosin-1 in renal glomeruli (Figure 2A). We also found that swiprosin-1 and CD31 co-localized in the glomeruli, which indicated that swiprosin-1 was primarily expressed in endothelial cells (Figure 2B). Moreover, Western blot results revealed that renal cortical swiprosin-1 expression increased markedly in a time-dependent manner after STZ-mediated diabetes mellitus induction (Figure 2C). Furthermore, we identified a significant augmentation of swiprosin-1 in diabetic GECs using immunofluorescence analysis (Figure 2D). Persistent hyperglycemia increased the expression of swiprosin-1 in GECs, whereas treatment with LY333531 reduced swiprosin-1 expression in the renal cortex and in GECs (Figure 2E and 2F) of diabetic mice. These data established that swiprosin-1 up-regulation was causally linked to experimental DN, and the activation of PKCβ was required for swiprosin-1 up-regulation in GECs.

PKCβ mediated a high-glucose-induced decrease in HRGEC viability and an increase in swiprosin-1 expression

We performed *in vitro* experiments to gain further insight into the mechanism of PKCβ-mediated GEC apoptosis. We observed the distribution of swiprosin-1 in HRGECs, and found that swiprosin-1 was co-localized with CD31-positive endothelial cells (Figure 3A), which confirmed the localization of swiprosin-1 in GECs *in vivo*. The viability of HRGECs was significantly impaired in medium containing high glucose (HG, 33 mmol/L) compared to cells cultured in normal glucose (NG, 5.5 mmol/L) after 24 h (Figure 3B). Lactate dehydrogenase (LDH), a marker of cytotoxicity, was also signifi-

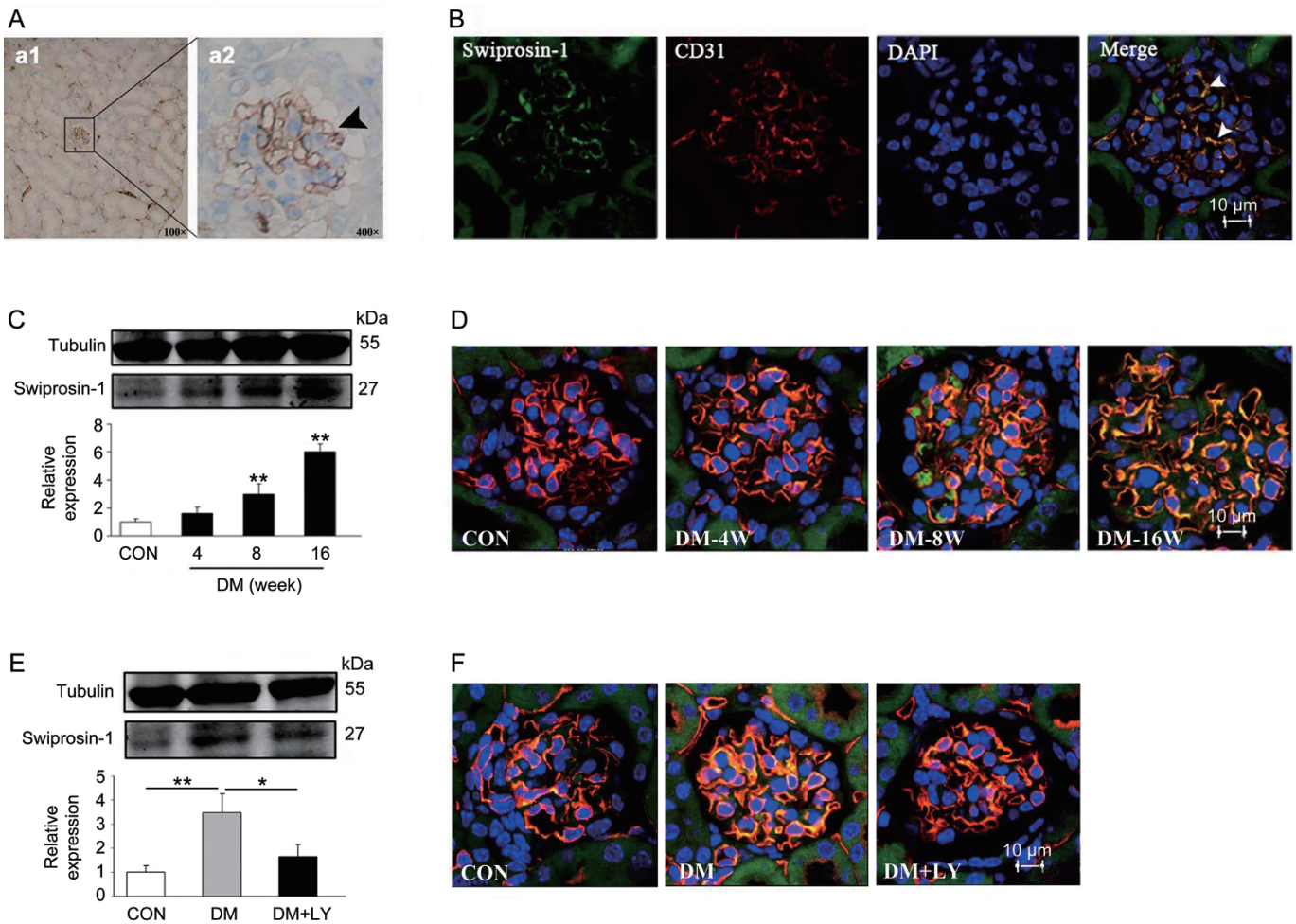

Figure 2. Swiprosin-1 expression was up-regulated by PKCβ activation in GECs of diabetic mice in the early stage of DN. (A) Immunohistochemistry and (B) immunofluorescence for swiprosin-1 (swiprosin-1: green; CD31: red; DAPI: blue) was performed in the glomeruli of C57BL/6 mice. (C) Immunoblot and (D) immunofluorescence for swiprosin-1 expression in GECs at 4, 8 and 16 weeks following STZ injection in C57BL/6 mice. (E) Immunoblot and (F) immunofluorescence for swiprosin-1 expression in GECs of diabetic mice treated with or without LY333531 (1 mg·kg^{-1}·d^{-1}) for 8 weeks. Images are representative of 5 mice in each group. Representative blots of three independent experiments are shown. $^{*}P<0.05$, $^{**}P<0.01$ compared with control or as indicated. Scale bar=10 μm. CON, control; DM, diabetes mellitus; LY, LY333531.

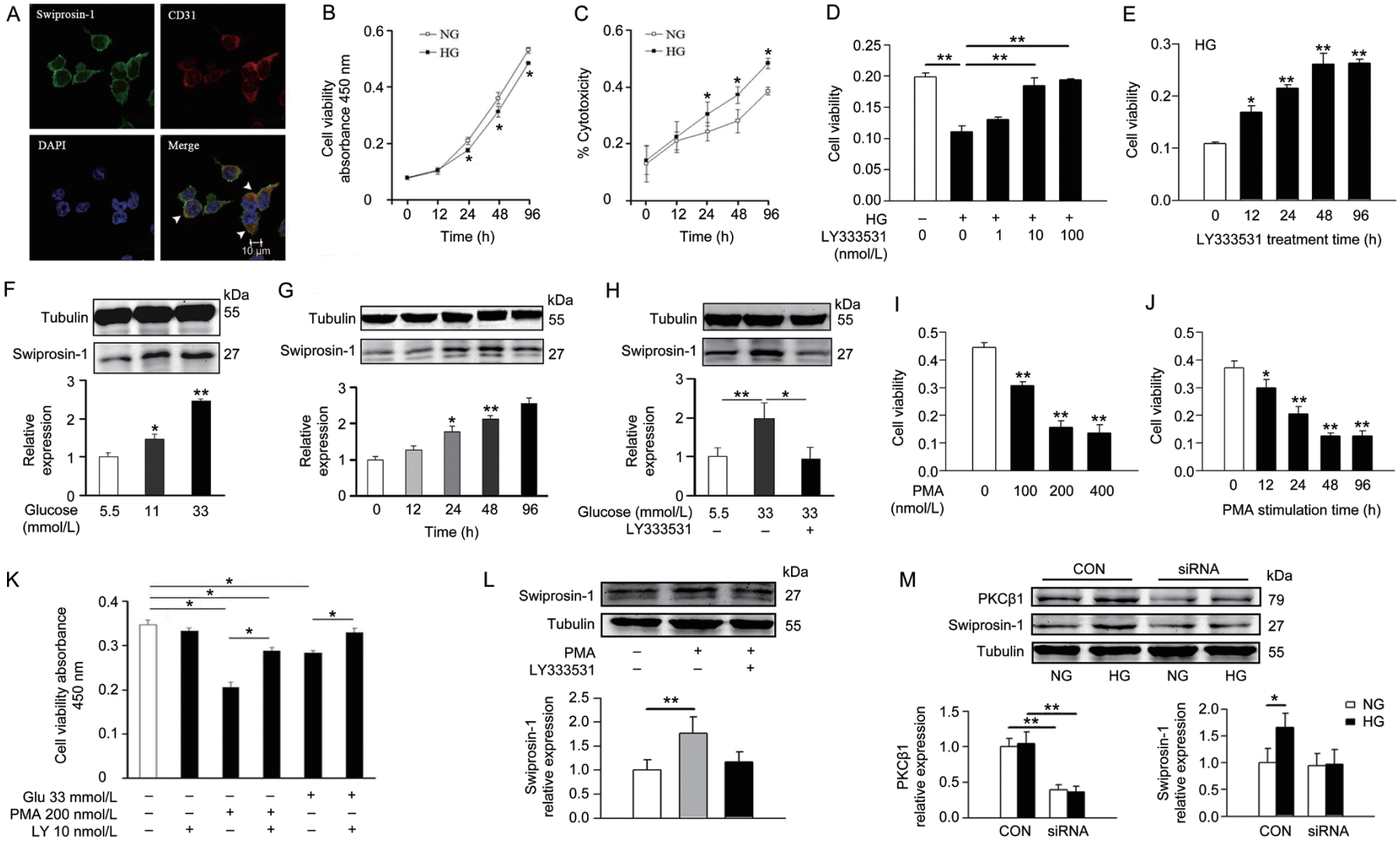

Figure 3. PKCβ-mediated decrease in HRGEC viability and increase in swiprosin-1 expression induced by high glucose. (A) Immunofluorescence for swiprosin-1 and CD31 in HRGECs. (B) Cell viability and (C) cytotoxicity of HRGECs treated with normal glucose (5.5 mmol) and high glucose (33 mmol). (D) Cell viability of HRGECs treated with different concentrations of LY333531 in a high-glucose environment. (E) Cell viability of HRGECs treated with 10 nmol/L LY333531 at different times in a high-glucose environment. (F) Immunoblot of swiprosin-1 expression in HRGECs treated with high glucose (11 mmol, 33 mmol) and normal glucose (5.5 mmol) for 48 h, (G) or treated with high glucose (33 mmol) for 0, 12, 24, 48, and 96 h. Immunoblot of swiprosin-1 (H) expression in HRGECs incubated with 5.5 mmol glucose, 33 mmol glucose, or 33 mmol glucose+10 nmol LY333531 for 48 h. Cell viability of HRGECs incubated with PMA at (I) different concentrations and (J) different time. (K) Cell viability of HRGECs was examined with different combinations of high glucose, PMA, and LY333531 for 48 h, as indicated. (L) Immunoblot of swiprosin-1 expression in HRGECs incubated with PMA (200 nmol/L) with or without LY333531 (10 nmol/L) for 48 h. (M) Expression of PKCβ1 and swiprosin-1 in *PKCβ*-targeted knockdown cells with or without incubation in high-glucose medium for 48 h. Representative blots of three independent experiments are shown. $^{*}P<0.05$, $^{**}P<0.01$ compared with NG (or control) group or as indicated. Scale bar=10 μm. NG, normal glucose; HG, high glucose; Glu, glucose; LY, LY333531.

cantly increased by HG stimulation (Figure 3C). LY333531 attenuated the HG-induced cell viability in a time- and dose-dependent fashion (Figure 3D and 3E). Treatment with LY333531 at 10 nmol/L for 48 h was the optimal experimental condition and was used in the following assays. We also observed that swiprosin-1 expression was dose- and time-dependently up-regulated under HG stimulation in HRGECs (Figure 3F and 3G), whereas LY333531 inhibited the increase in swiprosin-1 in HRGECs incubated with HG (Figure 3H).

PMA is a PKC agonist, and it also significantly decreased the viability of HRGECs in a time- and dose-dependent manner. Incubation with PMA at 200 nmol/L for 48 h caused a marked decrease in cell viability (Figure 3I and 3J). PMA or HG induced a decrease in HRGEC viability, whereas LY333531 normalized these changes (Figure 3K). Further, LY333531 soundly inhibited PMA-induced up-regulation of swiprosin-1 in HRGECs (Figure 3L). These *in vitro* findings were consistent with the normalization of GEC apoptosis in diabetic mice treated with LY333531. Furthermore, targeted knockdown of *PKCβ* using siRNA significantly inhibited HG-induced augmentation of swiprosin-1 (Figure 3M). Thus, PKCβ might mediate the up-regulation of swiprosin-1 in HRGECs induced by high glucose. These *in vitro* findings were consistent with those observed in GECs of diabetic mice *in vivo*.

Swiprosin-1 mediated the high-glucose-induced apoptosis of HRGECs

To investigate the possible effects of swiprosin-1 on high-glucose-induced HRGEC apoptosis, we constructed lentiviruses encoding shRNA targeting *swiprosin-1* (LV-sh-Swi) to knockdown swiprosin-1 and full-length *swiprosin-1* (LV-Swi) to over-express swiprosin-1. Over-expression of swiprosin-1 in HRGECs resulted in a significant decrease in cell viability (Figure 4A). The LV-Swi group showed an increase in the formation of pyknotic nuclei compared to the LV-GFP control group (Figure 4B). The results showed that the apoptosis rate of the swiprosin-1-over-expressing cells was two times higher than that of the control cells (18.96% *vs* 9.04%, Figure 4C).

Next, we observed the changes in swiprosin-1-knockdown cells. However, there was no significant difference in cell viability, pyknotic nuclei or apoptosis rate under normal medium between the LV-sh-GFP control group and LV-sh-Swi group (Figure 4D–4F). Hence, we compared the differences between these two groups in high-glucose conditions. The LV-sh-GFP-treated cells manifested a significant decrease in cell viability, a dramatic increase in the formation of pyknotic nuclei and an elevated apoptosis rate, from 7.47% to 25.37%, after HG stimulation (Figure 4D–4F). However, all these changes were abolished or attenuated with the knockdown of swiprosin-1 in HRGECs (Figure 4D–4F).

These data showed that increased swiprosin-1 expression induced by hyperglycemia contributed to HRGEC apoptosis. Thus, PKCβ might induce GEC apoptosis at the early stage of DN through up-regulation of swiprosin-1.

Swiprosin-1 mediated GEC apoptosis via the mitochondrial-dependent apoptotic pathway

We observed that the level of cleaved caspase-9 active fragment (39 and 37 kDa), cleaved caspase-3 active fragment (19 and 17 kDa), and Bax and the caspase-9 activity were significantly increased in swiprosin-1-over-expressing GECs (Figure 5A and 5C). The increase in cleaved caspase-9, cleaved caspase-3, Bax and caspase-9 activity in the LV-sh-Swi group treated with high glucose was remarkably attenuated compared with those in the LV-sh-GFP control group (Figure 5B and 5D). Additionally, immunoprecipitation results revealed that inactive procaspase-9 was increased and was associated with swiprosin-1 in the LV-Swi group (Figure 5E). Apaf-1 and cytochrome *c* are two important proteins required for caspase-9 activation[33, 34]. The interaction between swiprosin-1/procaspase-9, procaspase-9/Apaf-1 or procaspase-9/cytochrome *c* was significantly increased in cells transfected with LV-Swi. Moreover, immunofluorescence showed that swiprosin-1-over-expressing cells released more cytochrome *c* into the cytosol (Figure 5F).

In general, the pro-apoptotic protein Bax and a reduced level of the anti-apoptotic protein Bcl-2 can lead to an imbalance in the mitochondrial membrane potential. An increased ratio of Bax/Bcl-2 can result in mitochondrial release of cytochrome *c* into the cytosol, which is one of the early events in the onset of apoptosis[35]. We confirmed that PMA decreased cell viability and increased swiprosin-1 levels in HRGECs. Here, we assumed that the PMA-induced pro-apoptotic effect was produced via alteration of the Bax/Bcl-2 ratio and release of cytochrome *c* from the mitochondria into the cytosol. As the results show, PMA treatment resulted in a dose-dependent increase in the Bax/Bcl-2 ratio (Figure 6A), and cytochrome *c* was released from mitochondria into the cytosol in HRGECs after PMA exposure (Figure 6B). To validate whether the pro-apoptotic role of swiprosin-1 in PKC-activated HRGEC apoptosis occurred through the mitochondrial pathway, cells transfected with LV-sh-Swi were treated with PMA to observe the expression of the Bax/Bcl-2 ratio and subsequent changes in both mitochondrial and cytosolic cytochrome *c* expression. Western blot analysis results showed that knockdown of swiprosin-1 abolished the PMA-induced increase in the Bax/Bcl-2 ratio and the mitochondrial release of cytochrome *c* (Figure 6C and 6D). In addition, interfering with swiprosin-1 expression also inhibited the PMA-mediated increase in the expression of cleaved-caspase-9, cleaved-caspase-3 and cleaved PARP (substrate of active caspase-3). These results suggested that swiprosin-1 might mediate GEC apoptosis via the mitochondrial pathway, dependent on PKC activation.

Absence of swiprosin-1 abolished GEC apoptosis in diabetic mice

To further determine the effect of swiprosin-1 on GEC apoptosis *in vivo*, we compared STZ-induced diabetic *swiprosin-1*$^{+/+}$ mice with diabetic *swiprosin-1*$^{-/-}$ mice 8 weeks after induction. No difference was found in body weight, blood glucose or kidney/body weight between the swiprosin-1-knockout mice and wild-type mice under normal conditions (data not

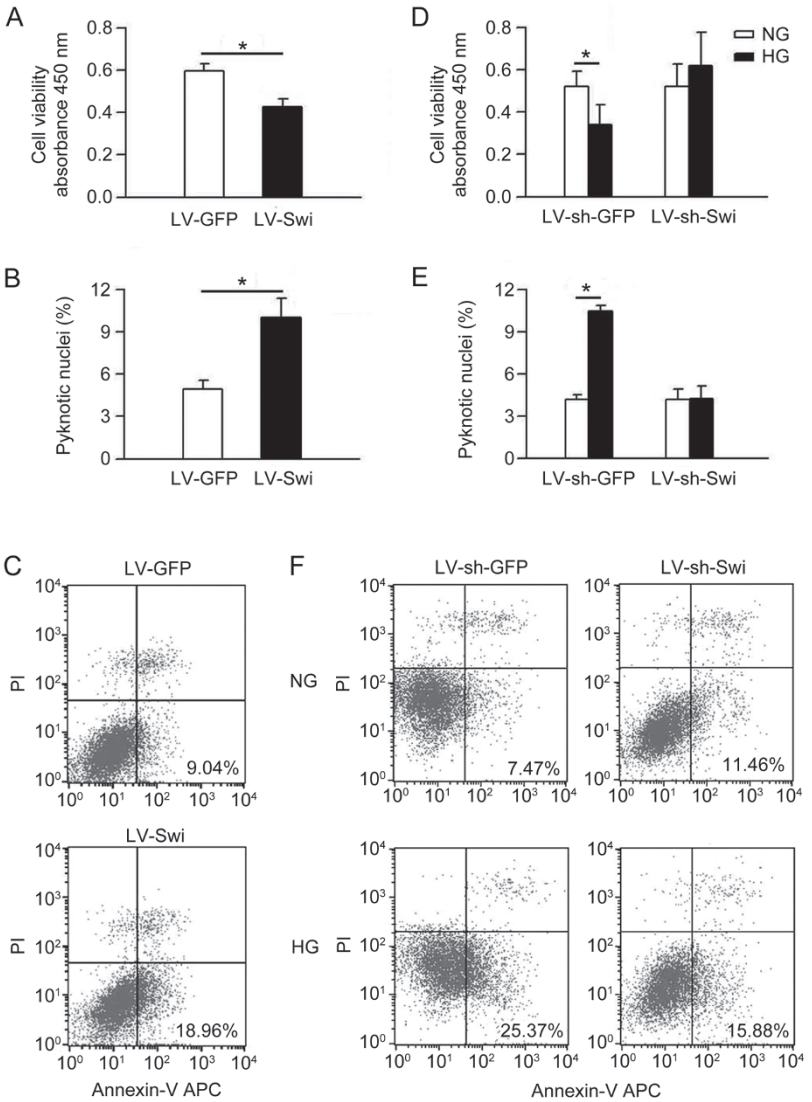

Figure 4. Swiprosin-1 mediated the apoptosis of HRGECs induced by high glucose. (A) Cell viability, (B) pyknotic nuclei, and (C) cell apoptosis rate of HRGECs transfected with lentivirus expressing full-length *swiprosin-1* (LV-Swi) were measured using a CCK-8 assay, Hoechst staining and an Annexin V-APC Apoptosis Analysis Kit. (D) Cell viability, (E) pyknotic nuclei, and (F) cell apoptosis rate of HRGECs transfected with lentivirus expressing shRNA of *swiprosin-1* (LV-sh-Swi) treated with normal glucose (5.5 mmol) or high glucose (33 mmol) for 48 h were measured. $^{*}P<0.05$ compared as indicated. NG, normal glucose; HG, high glucose.

shown). However, diabetic *swiprosin-1*$^{-/-}$ mice exhibited a significant increase in serum CST3 and a decrease in kidney/body weight and urinary albumin compared with diabetic *swiprosin-1*$^{+/+}$ mice (Table 3). Additionally, extracellular matrix deposition in glomeruli and glomerular hypertrophy were significantly exacerbated in diabetic *swiprosin-1*$^{+/+}$ mice compared with diabetic *swiprosin-1*$^{-/-}$ mice (Figure 7A and 7B). We also observed TUNEL staining in CD31-positive cells and found that the apoptosis rate of GECs in diabetic *swiprosin-1*$^{+/+}$ mice increased significantly compared with that in *swiprosin-1*$^{+/+}$ control mice, while differences in the number of apoptotic GECs in *swiprosin-1*$^{-/-}$ diabetic mice were not obviously different compared with those in *swiprosin-1*$^{-/-}$ control mice (Figure 7C). Next, we determined the changes in mitochondrial-associated apoptotic molecules in the renal cortex of diabetic mice treated with LY333531 or in *swiprosin-1*$^{-/-}$ diabetic mice. As the results show, LY333531 significantly decreased the expression of PARP, cleaved-caspase9, and cleaved-caspase3, as well as the Bax/Bcl-2 ratio, in diabetic mice (Figure 7D). Additionally, increased levels of cleaved caspase-9 and cleaved caspase-3 and the elevated Bax/Bcl-2 ratio were also abolished in *swiprosin-1*$^{-/-}$ diabetic mice (Figure 7E).

Taken together, these results indicated that GEC apoptosis in the early stage of DN is associated with up-regulation of swiprosin-1, which is activated by PKCβ. Swiprosin-1 then promotes GEC apoptosis in DN via the mitochondrial pathway (Figure 7F).

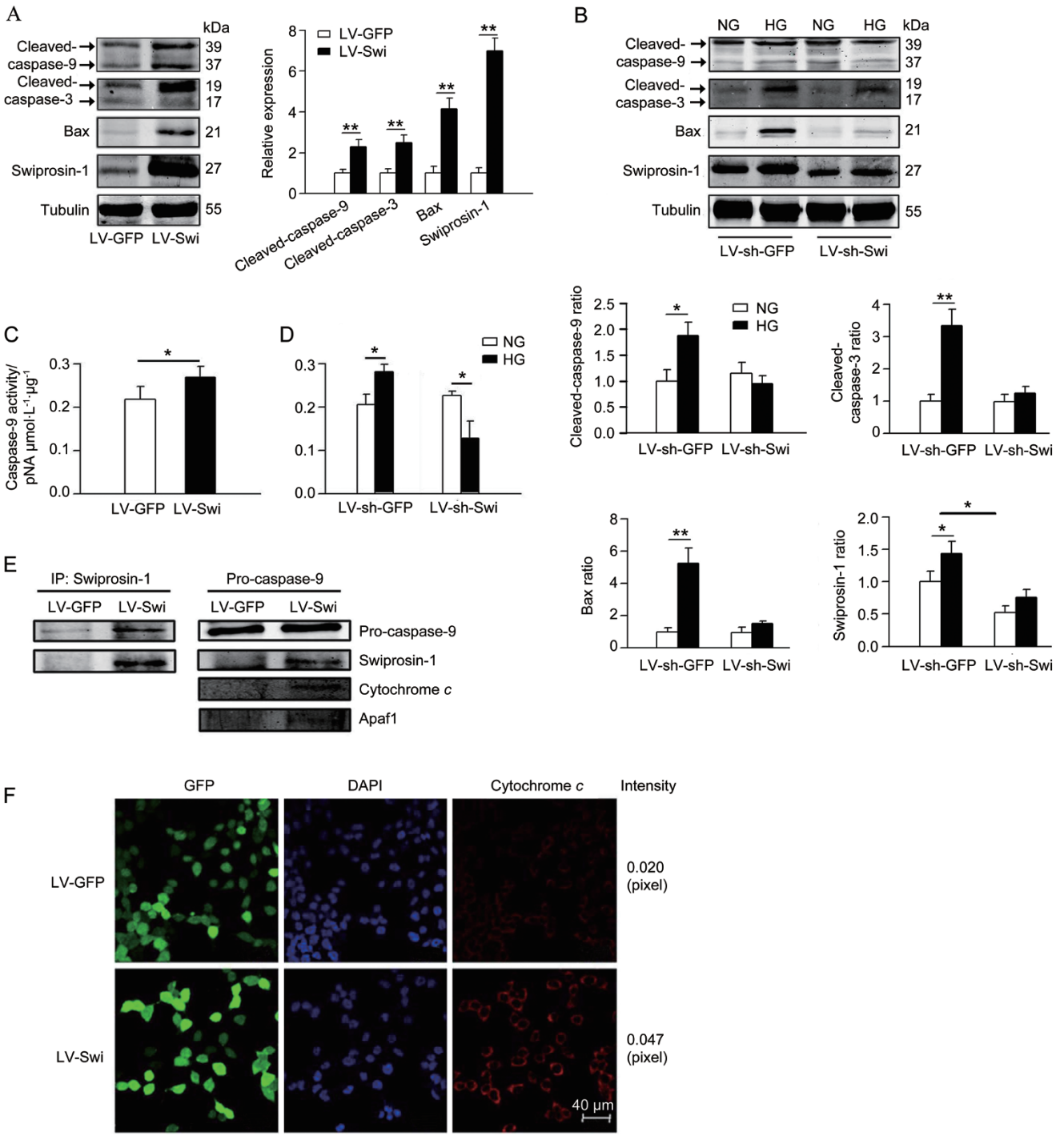

Figure 5. Swiprosin-1 mediated high-glucose-induced HRGEC apoptosis via caspase-9. (A) Expression of swiprosin-1, cleaved caspase-9, cleaved caspase-3 and Bax and (C) caspase-9 activity in HRGECs transfected with lentivirus expressing full-length *swiprosin-1* (LV-Swi, LV-GFP as control). (B) Expression of swiprosin-1, cleaved caspase-9, cleaved caspase-3 and Bax and (D) caspase-9 activity in HRGECs transfected with lentivirus expressing shRNA of *swiprosin-1* (LV-sh-Swi, LV-sh-GFP as control) treated with NG (5.5 mmol) or HG (33 mmol). (E) Left panels: The cell lysates were incubated with anti-swiprosin-1 antibody, and the immunoprecipitates were subjected to immunoblot by anti-swiprosin-1 antibody and anti-procaspase-9 antibody. Right panels: The cell lysates were incubated with anti-procaspase-9 antibody, and the immunoprecipitates were subjected to immunoblot with primary antibody against procaspase-9, swiprosin-1, cytochrome *c* and Apaf-1. (F) Release of cytochrome *c* in HRGECs transfected either with empty vector or with LV-Swi was analyzed by immunofluorescence using an anti-cytochrome *c* antibody. Representative immunofluorescence images of cytochrome *c* (red) are shown. Representative blots of three independent experiments are shown. $^{*}P<0.05$, $^{**}P<0.01$ compared as indicated. Scale bar=40 μm. NG, normal glucose; HG, high glucose.

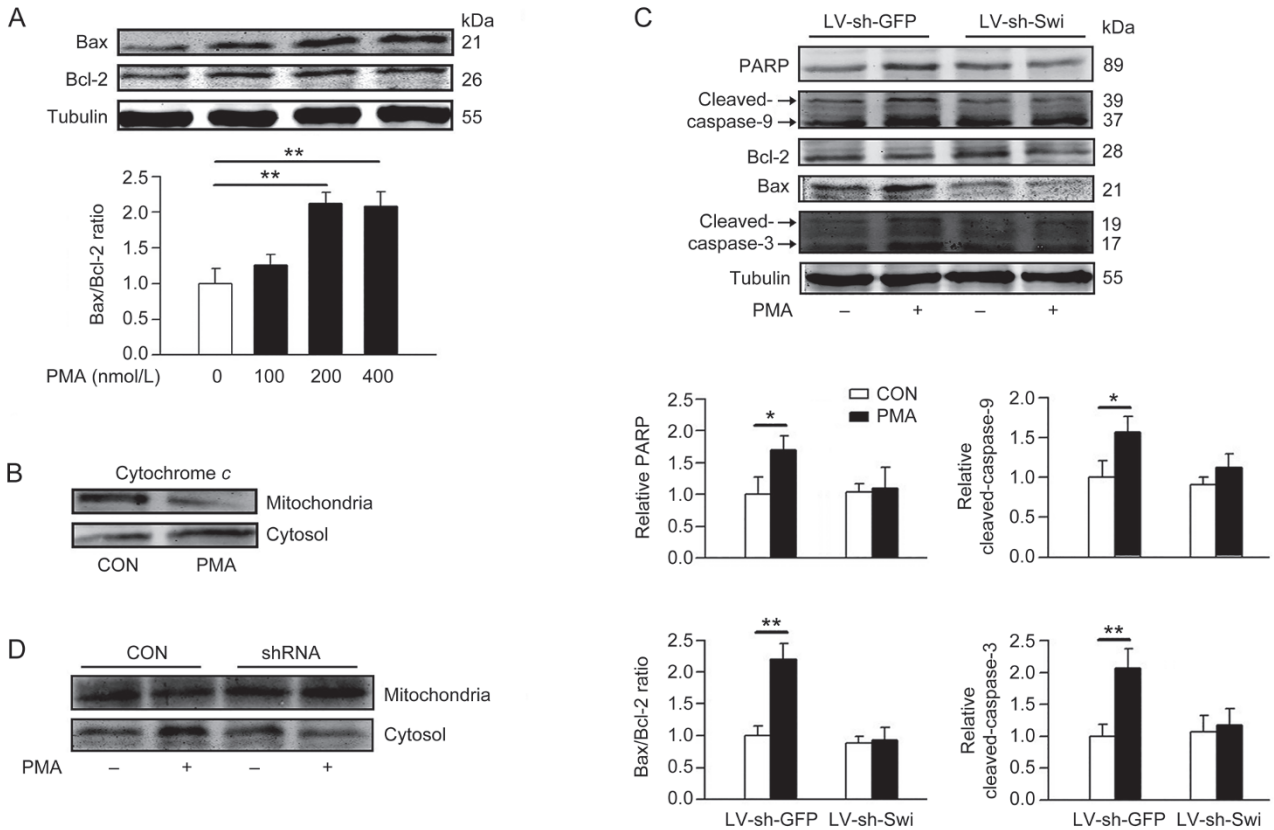

Figure 6. Swiprosin-1 mediated PMA-induced HRGEC apoptosis via the mitochondrial-dependent pathway. (A) Bax/Bcl-2 ratio changes when HRGECs are incubated in different concentrations of PMA. (B) Cytochrome *c* expression in the mitochondria and cytosol under PMA stimulation. (C) Expression of PARP, cleaved-caspase 9, cleaved-caspase 3 and Bax/Bcl-2 in *swiprosin-1*-knockdown cells with or without PMA incubation. (D) Expression of mitochondrial and cytosolic cytochrome *c* in *swiprosin-1*-knockdown cells with or without PMA incubation. Representative blots of three independent experiments are shown. $^{*}P<0.05$, $^{**}P<0.01$ compared as indicated. CON, control.

Discussion

In the current study, we found that a PKCβ inhibitor significantly reduced GEC apoptosis in diabetic mice. We demonstrated that swiprosin-1 expression was up-regulated by PKCβ in the early stage of DN or in HRGECs induced by high glucose or PMA. We also found that swiprosin-1 mediated GEC apoptosis through the mitochondrial-dependent pathway. These results suggest that activation of PKCβ can enhance swiprosin-1 expression to mediate GEC apoptosis in the early stage of DN.

Previous studies have shown that activation of PKCβ contributed to high-glucose-induced renal hypertrophy and extracellular matrix expansion[14, 16]. Koya *et al* showed that administration of LY333531 inhibited glomerular PKCβ activation and reduced urinary albumin excretion rates and mesangial expansion in diabetic *db*/*db* mice[16, 36]. In addition, increased type IV collagen production evoked by high glucose *in vitro* was prevented by a PKCβ inhibitor in cultured mesangial cells[37]. Although numerous studies *in vivo* and *in vitro* have indicated that a PKCβ inhibitor can protect against DN, the effect of PKCβ inhibition on diabetic GECs *in vivo* has not been previously examined. Clinical studies in patients with type 2 DM reported apoptosis of GECs and other glomerular cells that were associated with the progression of glomerular diabetic lesions[38]. Here, we found that LY333531 attenuated hyperglycemia-induced GEC apoptosis and ameliorated the inhibition of HRGEC viability caused by PMA or high glucose. Our findings provide evidence that inhibition of PKCβ activity in renal glomeruli can ameliorate GEC apoptosis in the early stage of DN.

Swiprosin-1 was detected in the spleen, lung and liver, with the highest abundance in the brain and the lowest abundance in the kidney and thymus[18]. The protein atlas database showed that swiprosin-1 has a medium expression level in human renal glomeruli but is not expressed in tubules. In accordance with these data, we demonstrated that swiprosin-1 was expressed in glomeruli, with medium expression in GECs. In addition, it was reported that swiprosin-1 could be up-regulated through the PKC β_1/η pathway in mast cells[19]. Here, we demonstrated that the expression of swiprosin-1 was up-regulated in GECs of diabetic mice *in vivo* as well as in HRGECs treated with high glucose or PMA *in vitro*. Moreover, the increase in swiprosin-1 expression in GECs under diabetic conditions could be ameliorated by LY333531 or

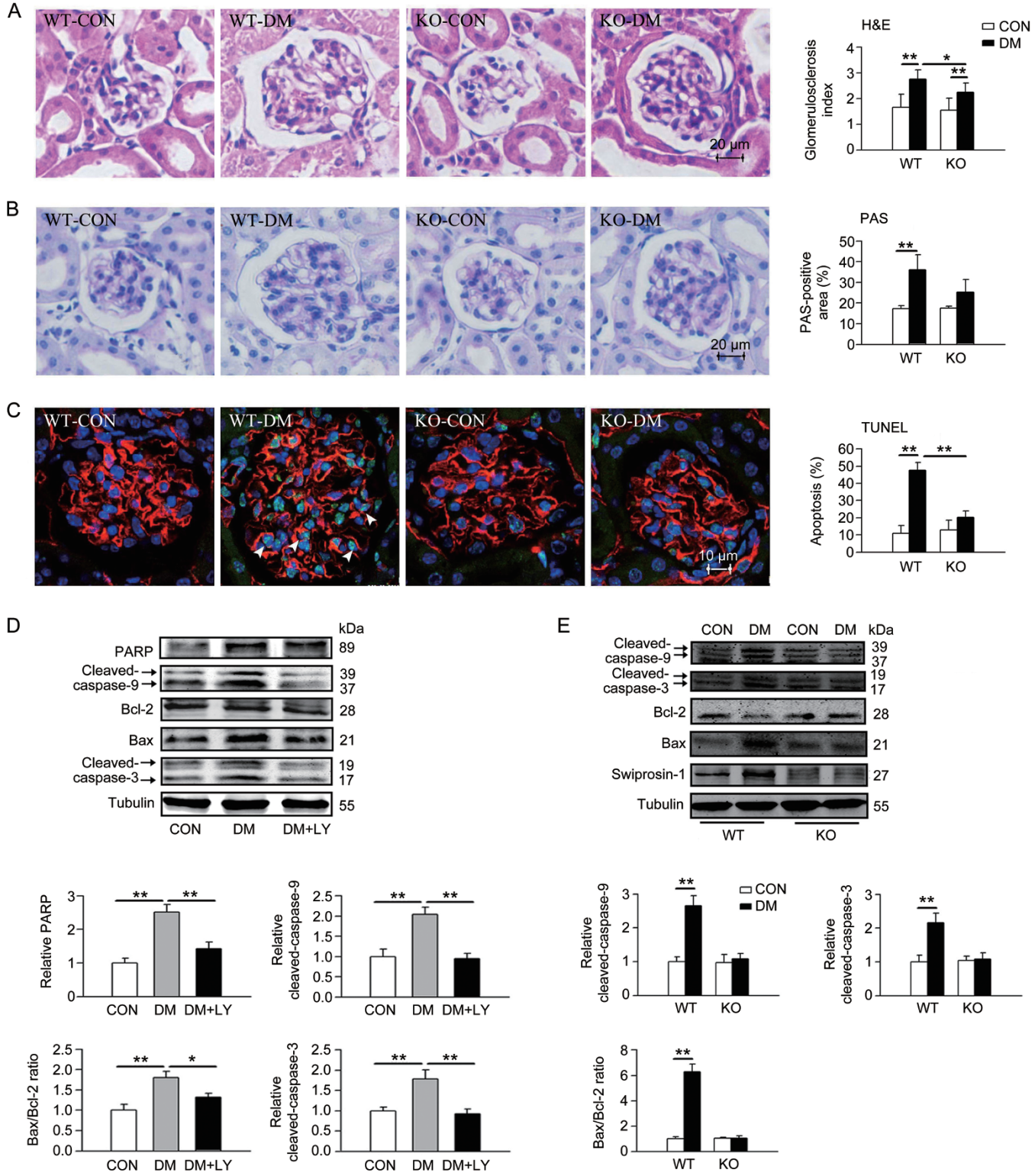

Figure 7A–7E. Abolishment of swiprosin-1 attenuated GEC apoptosis induced by diabetes. (A) H&E staining, (B) PAS staining, and (C) TUNEL staining were used to observed glomerular volume, extracellular matrix deposition, and GEC apoptosis in glomeruli of nondiabetic *swiprosin-1*$^{+/+}$ mice (wild type, WT-CON), diabetic *swiprosin-1*$^{+/+}$ mice (WT-DM), nondiabetic *swiprosin-1*$^{-/-}$ mice (knockout, KO-CON) and diabetic *swiprosin-1*$^{-/-}$ mice (KO-DM) at 8 weeks. TUNEL-stained fluorescein-labeled nucleotides (green), CD31 (red), and DAPI nuclear counterstain (blue). The changes in mitochondria-associated apoptotic molecules in the renal cortex of diabetic mice treated with (D) LY333531 or (E) *swiprosin-1*$^{-/-}$ diabetic mice. Representative blots of three independent experiments are shown. $^{*}P<0.05$, $^{**}P<0.01$ compared as indicated. Scale bar=20 μm in H&E and PAS staining; scale=10 μm in TUNEL staining. CON, control; DM, diabetes mellitus; LY, LY333531; WT, wild type; KO, knockout.

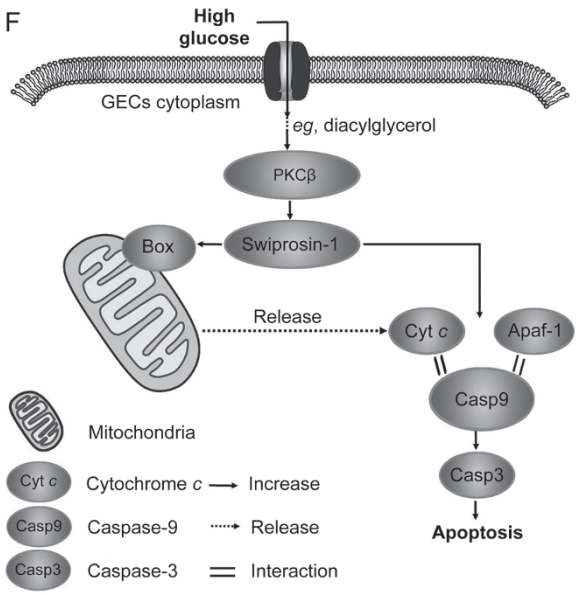

Figure 7F. High glucose induced up-regulation of swiprosin-1 expression through the activation of PKCβ and then triggered GEC apoptosis via the mitochondrial-dependent apoptosis pathway.

targeted knockdown of *PKCβ*. Our results confirmed that swiprosin-1 expression was regulated by PKCβ in GECs.

It was also reported that swiprosin-1 could promote cell apoptosis[18, 39]. Hence, it is likely that GEC apoptosis induced by high glucose may depend on swiprosin-1. Therefore, it is critical to identify the pro-apoptotic properties of swiprosin-1 in GECs in DN. Over-expression of swiprosin-1 in HRGECs resulted in a significant decrease in cell viability and an increase in the formation of pyknotic nuclei and the rate of apoptosis. In contrast, knockdown of swiprosin-1 attenuated GEC apoptosis induced by high glucose or PMA. These results identified a pro-apoptotic effect of swiprosin-1 on GECs in DN. Specifically, swiprosin-1 deficiency could ameliorate GEC apoptosis, kidney/body weight, urinary albumin, glomerular filtration rate, extracellular matrix deposition and glomerular hypertrophy in the early stage of DN. In addition, notably, the severity of DN and apoptosis of GECs were significantly diminished in diabetic *swiprosin-1*$^{-/-}$ mice. These results demonstrated that the pro-apoptotic role of swiprosin-1 expressed in GECs possibly aggravates DN. However, whether the effect of swiprosin-1 is endothelial cell-dependent is unclear, and future studies using a GEC conditional knockout model are highly necessary.

Ectopic expression of swiprosin-1 in immature B-cells enhanced BCR-induced apoptosis, with loss of the mitochondrial membrane potential, indicating that swiprosin-1 might induce apoptosis through the mitochondrial pathway. Swiprosin-1 was found to be associated with the caspase-9 protein complex, indicating that swiprosin-1 might act as a caspase substrate or a regulator of caspase-9 dependent apoptosis[39]. Caspase-9, which initiates the mitochondria-dependent apoptotic cascade, is synthesized as an inactive monomer and is activated after binding to Apaf-1, subsequently forming the apoptosome in the presence of cytochrome c[40]. This dimerization induces activation of caspase-9, which selectively cleaves a restricted set of target proteins with a weight of 39 kDa or 37 kDa and then directly activates caspase-3. Caspase-3 then commits the cell to apoptosis[41]. To gain insight into the role of the swiprosin-1-dependent apoptotic effect in diabetic GECs, we determined the increase in the levels of the caspase-9 active fragment and caspase-3 active fragment and in the caspase-9 activity. The results indicated that swiprosin-1-mediated apoptosis in HRGECs might depend on caspase-9.

The mitochondrial-dependent apoptosis pathway relies on the B-cell lymphoma 2 (Bcl-2) family to regulate cell death[40]. The Bcl-2 family controls the integrity of the outer mitochondrial membrane, and it is functionally divided into anti- and pro-apoptotic proteins[42]. Bax (one of the pro-apoptotic Bcl-2 family members) forms proteolipid pores within the outer mitochondrial membrane, resulting in the release of cytochrome c into the cytosol[43, 44]. The released cytochrome c associates with the cytosolic protein Apaf-1 and procaspase-9 to form the apoptosome[45]. Our co-immunoprecipitation experiment revealed that swiprosin-1 augmented caspase-9/cytochrome c and caspase-9/Apaf-1 interactions. In addition, the interaction between swiprosin-1 and caspase-9 could also be intensified by high glucose. Furthermore, our study showed that swiprosin-1 increased the Bax/Bcl-2 ratio and facilitated cytochrome c release from mitochondria. These results demonstrated that swiprosin-1 modulated GEC apoptosis through the mitochondrial apoptotic pathway.

In conclusion, our study demonstrated that swiprosin-1 expression was up-regulated by PKCβ, which then facilitated GEC apoptosis through the mitochondrial-dependent pathway in the early stage of DN. Therefore, our findings are the first to highlight the important role of swiprosin-1 in GEC apoptosis in the early stage of DN and provide new evidence for the application of a PKCβ inhibitor for the treatment of DN.

Acknowledgements

We thank Tong-hui MA (Dalian Medical University, China) and Wei-heng SU (Jilin University, China) for constructing the swiprosin-1 knockout mouse. This study was supported by grants from the National Natural Science Foundation of China (No 81273504, 81473258 and 81402941), the Shanghai Municipal Commission of Health and Family Planning (No 20144Y0204 and 201540294), the Science and Technology Commission of Shanghai Municipality (No 15140904600), and the Natural Science Foundation of Shanghai (No 16ZR1434400).

Author contribution

Zhi-bin WANG, Ya LI, and Ye TU contributed to the conception and design of the study, and performed the research; Ling-chang TONG, Yue WANG, Wei-ye LIU, Rong-mei WANG, and Su ZHANG contributed to the acquisition, analysis and interpretation of data; Zhi-bin WANG drafted the manuscript. Ling LI, Li-chao ZHANG, and Ding-feng SU supervised the project and revised the manuscript critically for important

intellectual content. All authors have approved the final vision of this manuscript.

References

1 Kei A, Liberopoulos E, Elisaf M. Effect of hypolipidemic treatment on glycemic profile in patients with mixed dyslipidemia. World J Diabetes 2013; 4: 365–71.
2 Gruden G, Barutta F, Kunos G, Pacher P. Role of the endocannabinoid system in diabetes and diabetic complications. Br J Pharmacol 2016; 173: 1116–27.
3 Isermann B, Vinnikov IA, Madhusudhan T, Herzog S, Kashif M, Blautzik J, *et al*. Activated protein C protects against diabetic nephropathy by inhibiting endothelial and podocyte apoptosis. Nat Med 2007; 13: 1349–58.
4 Satchell SC. The glomerular endothelium emerges as a key player in diabetic nephropathy. Kidney Int 2012; 82: 949–51.
5 Schlondorff D, Banas B. The mesangial cell revisited: no cell is an island. J Am Soc Nephrol 2009; 20: 1179–87.
6 Chen YQ, Wang XX, Yao XM, Zhang DL, Yang XF, Tian SF, *et al*. Abated microRNA-195 expression protected mesangial cells from apoptosis in early diabetic renal injury in mice. J Nephrol 2012; 25: 566–76.
7 Menini S, Iacobini C, Oddi G, Ricci C, Simonelli P, Fallucca S, *et al*. Increased glomerular cell (podocyte) apoptosis in rats with streptozotocin-induced diabetes mellitus: role in the development of diabetic glomerular disease. Diabetologia 2007; 50: 2591–9.
8 Riedl E, Pfister F, Braunagel M, Brinkkotter P, Sternik P, Deinzer M, *et al*. Carnosine prevents apoptosis of glomerular cells and podocyte loss in STZ diabetic rats. Cell Physiol Biochem 2011; 28: 279–88.
9 Zhang L, Li R, Shi W, Liang X, Liu S, Ye Z, *et al*. NFAT2 inhibitor ameliorates diabetic nephropathy and podocyte injury in *db/db* mice. Br J Pharmacol 2013; 170: 426–39.
10 Nakagawa T, Tanabe K, Croker BP, Johnson RJ, Grant MB, Kosugi T, *et al*. Endothelial dysfunction as a potential contributor in diabetic nephropathy. Nat Rev Nephrol 2011; 7: 36–44.
11 Maezawa Y, Takemoto M, Yokote K. Cell biology of diabetic nephropathy: Roles of endothelial cells, tubulointerstitial cells and podocytes. J Diabetes Investig 2015; 6: 3–15.
12 Li J, Gobe G. Protein kinase C activation and its role in kidney disease. Nephrology (Carlton) 2006; 11: 428–34.
13 Teng B, Duong M, Tossidou I, Yu X, Schiffer M. Role of protein kinase C in podocytes and development of glomerular damage in diabetic nephropathy. Front Endocrinol (Lausanne) 2014; 5: 179.
14 Noh H, King GL. The role of protein kinase C activation in diabetic nephropathy. Kidney Int Suppl 2007; (106): S49–53.
15 Meier M, Park JK, Overheu D, Kirsch T, Lindschau C, Gueler F, *et al*. Deletion of protein kinase C-beta isoform *in vivo* reduces renal hypertrophy but not albuminuria in the streptozotocin-induced diabetic mouse model. Diabetes 2007; 56: 346–54.
16 Ohshiro Y, Ma RC, Yasuda Y, Hiraoka-Yamamoto J, Clermont AC, Isshiki K, *et al*. Reduction of diabetes-induced oxidative stress, fibrotic cytokine expression, and renal dysfunction in protein kinase Cbeta-null mice. Diabetes 2006; 55: 3112–20.
17 Vuadens F, Rufer N, Kress A, Corthesy P, Schneider P, Tissot JD. Identification of swiprosin 1 in human lymphocytes. Proteomics 2004; 4: 2216–20.
18 Avramidou A, Kroczek C, Lang C, Schuh W, Jack HM, Mielenz D. The novel adaptor protein Swiprosin-1 enhances BCR signals and contributes to BCR-induced apoptosis. Cell Death Differ 2007; 14: 1936–47.
19 Thylur RP, Kim YD, Kwon MS, Oh HM, Kwon HK, Kim SH, *et al*. Swiprosin-1 is expressed in mast cells and up-regulated through the protein kinase C beta I/eta pathway. J Cell Biochem 2009; 108: 705–15.
20 Tomic MA, Vuckovic SM, Stepanovic-Petrovic RM, Micov AM, Ugresic ND, Prostran MS, *et al*. Analysis of the antinociceptive interactions in two-drug combinations of gabapentin, oxcarbazepine and amitriptyline in streptozotocin-induced diabetic mice. Eur J Pharmacol 2010; 628: 75–82.
21 Wei N, Yu SP, Gu XH, Chen DD, Whalin MK, Xu GL, *et al*. The involvement of autophagy pathway in exaggerated ischemic brain damage in diabetic mice. CNS Neurosci Ther 2013; 19: 753–63.
22 Koyama N, Nishida Y, Ishii T, Yoshida T, Furukawa Y, Narahara H. Telmisartan induces growth inhibition, DNA double-strand breaks and apoptosis in human endometrial cancer cells. PLoS One 2014; 9: e93050.
23 Guo S, Xiao D, Liu H, Zheng X, Liu L, Liu S. Interfering with CXCR4 expression inhibits proliferation, adhesion and migration of breast cancer MDA-MB-231 cells. Oncol Lett 2014; 8: 1557–62.
24 Mishra R, Emancipator SN, Kern T, Simonson MS. High glucose evokes an intrinsic proapoptotic signaling pathway in mesangial cells. Kidney Int 2005; 67: 82–93.
25 Song S, Wang S, Ma J, Yao L, Xing H, Zhang L, *et al*. Biliverdin reductase/bilirubin mediates the anti-apoptotic effect of hypoxia in pulmonary arterial smooth muscle cells through erk1/2 pathway. Exp Cell Res 2013; 319: 1973–87.
26 Song S, Meyer M, Turk TR, Wilde B, Feldkamp T, Assert R, *et al*. Serum cystatin C in mouse models: a reliable and precise marker for renal function and superior to serum creatinine. Nephrol Dial Transplant 2009; 24: 1157–61.
27 Isobe K, Adachi K, Hayashi S, Ito T, Miyoshi A, Kato A, *et al*. Spontaneous glomerular and tubulointerstitial lesions in common marmosets (callithrix jacchus). Veterinary Pathol 2012; 49: 839–45.
28 Liu WY, Wang ZB, Wang Y, Tong LC, Li Y, Wei X, *et al*. Increasing the permeability of the blood-brain barrier in three different models *in vivo*. CNS Neurosci Ther 2015; 21: 568–74.
29 Avens HJ, Berron BJ, May AM, Voigt KR, Seedorf GJ, Balasubramaniam V, *et al*. Sensitive immunofluorescent staining of cells via generation of fluorescent nanoscale polymer films in response to biorecognition. J Histochem Cytochem 2011; 59: 76–87.
30 Verhoest G, Dolley-Hitze T, Jouan F, Belaud-Rotureau MA, Oger E, Lavenu A, *et al*. Sunitinib combined with angiotensin-2 type-1 receptor antagonists induces more necrosis: a murine xenograft model of renal cell carcinoma. Biomed Res Int 2014; 2014: 901371.
31 Li ST, Pan J, Hua XM, Liu H, Shen S, Liu JF, *et al*. Endothelial nitric oxide synthase protects neurons against ischemic injury through regulation of brain-derived neurotrophic factor expression. CNS Neurosci Ther 2014; 20: 154–64.
32 Peng Y, Li L, Huang M, Duan C, Zhang L, Chen J. Angiogenin interacts with ribonuclease inhibitor regulating PI3K/AKT/mTOR signaling pathway in bladder cancer cells. Cell Signal 2014; 26: 2782–92.
33 Li P, Nijhawan D, Budihardjo I, Srinivasula SM, Ahmad M, Alnemri ES, *et al*. Cytochrome *c* and dATP-dependent formation of Apaf-1/caspase-9 complex initiates an apoptotic protease cascade. Cell 1997; 91: 479–89.
34 Zou H, Henzel WJ, Liu X, Lutschg A, Wang X. Apaf-1, a human protein homologous to *C. elegans* CED-4, participates in cytochrome c-dependent activation of caspase-3. Cell 1997; 90: 405–13.
35 Habibovic S, Hrgovic Z, Bukvic I, Hrgovic I. Molecular mechanisms in apoptosis. Med Arh 2000; 54: 33–40.
36 Koya D, Haneda M, Nakagawa H, Isshiki K, Sato H, Maeda S, *et al*. Amelioration of accelerated diabetic mesangial expansion by

treatment with a PKC beta inhibitor in diabetic *db/db* mice, a rodent model for type 2 diabetes. FASEB J 2000; 14: 439–47.
37 Cohen MP, Ziyadeh FN, Lautenslager GT, Cohen JA, Shearman CW. Glycated albumin stimulation of PKC-beta activity is linked to increased collagen IV in mesangial cells. Am J Physiol 1999; 276: F684–90.
38 Verzola D, Gandolfo MT, Ferrario F, Rastaldi MP, Villaggio B, Gianiorio F, *et al*. Apoptosis in the kidneys of patients with type II diabetic nephropathy. Kidney Int 2007; 72: 1262–72.
39 Checinska A, Giaccone G, Rodriguez JA, Kruyt FA, Jimenez CR. Comparative proteomics analysis of caspase-9-protein complexes in untreated and cytochrome c/dATP stimulated lysates of NSCLC cells. J Proteomics 2009; 72: 575–85.
40 Wang X. The expanding role of mitochondria in apoptosis. Genes Dev 2001; 15: 2922–33.
41 Estaquier J, Vallette F, Vayssiere JL, Mignotte B. The mitochondrial pathways of apoptosis. Adv Exp Med Biol 2012; 942: 157–83.
42 Harris MH, Thompson CB. The role of the Bcl-2 family in the regulation of outer mitochondrial membrane permeability. Cell Death Differ 2000; 7: 1182–91.
43 Gross A, McDonnell JM, Korsmeyer SJ. BCL-2 family members and the mitochondria in apoptosis. Genes Dev 1999; 13: 1899–911.
44 Higgins GC, Coughlan MT. Mitochondrial dysfunction and mitophagy: the beginning and end to diabetic nephropathy? Br J Pharmacol 2014; 171: 1917–42.
45 McIlwain DR, Berger T, Mak TW. Caspase functions in cell death and disease. Cold Spring Harb Perspect Biol 2015; 7. pii: a026716.